

## An Improved MCB Localization Algorithm Based on Weighted RSSI and Motion Prediction

Chunyue Zhou<sup>1</sup>, Hui Tian<sup>2</sup>, and Baitong Zhong<sup>3</sup>

<sup>1</sup> Laboratory of Communication Engineering  
Beijing Jiaotong University, China  
zhouchunyue@hotmail.com

<sup>2</sup> School of Information and Communication Technology  
Griffith University, Australia  
hui.tian@griffith.edu.au

<sup>3</sup> Hunan Electronic Technology Vocational College  
Hunan Province, China  
471727138@qq.com

**Abstract.** Aiming at the problem of low sampling efficiency and high demand for anchor node density of traditional Monte Carlo Localization Boxed algorithm, an improved algorithm based on historical anchor node information and the received signal strength indicator (RSSI) ranging weight is proposed which can effectively constrain sampling area of the node to be located. Moreover, the RSSI ranging of the surrounding anchors and the neighbor nodes is used to provide references for the position sampling weights of the nodes to be located, an improved motion model is proposed to further restrict the sampling area in direction. The simulation results show that the improved Monte Carlo Localization Boxed (IMCB) algorithm effectively improves the accuracy and efficiency of localization.

**Keywords:** Wireless sensor networks, Localization, Monte Carlo Boxed, RSSI, Motion prediction.

### 1. Introduction

Wireless sensor networks (WSN) is a wireless communication network system that integrates monitoring, control, wireless communication and other functions. With the development of wireless sensor network technology, sensors are widely used in environment, military, medical, space exploration and many other fields. In these applications, the location of sensor nodes is a very important information, locating technology has become the key support technology of wireless sensor networks. With the diversification of wireless sensor network applications and the gradual maturity of static network node locating technology, mobile node locating technology has attracted more and more attention in recent years.

The localization algorithm of wireless sensor network nodes can be divided into localization algorithm based on ranging and localization algorithm based on non-ranging. Ranging-based localization algorithm is based on AOA [1], TOA [2], TDOA [3], RSSI [4] and other ranging technologies to obtain the distance between ordinary

nodes and anchor nodes, and then use spatial geometry rules to calculate the location of unknown nodes through triangular localization algorithm, trilateral localization algorithm, multilateral localization algorithm, maximum likelihood estimation algorithm, etc. Non-ranging localization algorithm does not need to measure the distance between nodes, but calculates the location of unknown nodes by calculating the connectivity between unknown nodes and surrounding nodes, such as centroid localization [5], DV-Hop localization [6], convex programming [7], APIT [8], etc.

Fixed wireless sensor network node localization algorithms are numerous and relatively mature, but the complexity of mobile node localization algorithm leads to a huge amount of computation, and the localization accuracy is also deficient, so it is an urgent need for a location strategy suitable for mobile sensor networks.

In [9], Hu and Evans proposed a Monte Carlo-based mobile wireless sensor network node localization algorithm-MCL for node location of wireless mobile sensor networks. The algorithm proposes a simulation-based solution to estimate the posterior probability distribution of nonlinear discrete-time motion models. In view of the low efficiency of position sampling of the MCL algorithm, many improved mobile node localization algorithms have been developed based on MCL, such as Monte Carlo Localization Boxed algorithm (MCB) [10], range-based-MCL algorithm [11], RSSI-MCL algorithm [12], etc. The MCB algorithm establishes the sampling range of the anchor box limit position prediction by making full use of the one-hop (two-hop) anchor node information that the unknown node can perceive, which effectively improves the accuracy and efficiency of the node positioning [13]. However, the MCB still has a large and fuzzy sampling point set, and there is also much room for improvement in the prediction of the motion direction of the node. In addition to the above improved strategies, there are many researches on the localization algorithm of wireless mobile sensor networks based on Monte Carlo localization algorithm, such as adaptive weight [14], virtual anchor node [15], model prediction [16], fusion posture estimation [17] etc. Aiming at the problem of MCB algorithm, this paper proposes an improved MCB for mobile sensor networks. The algorithm further limits the sampling range of the nodes to be located by using the historical anchor node and its RSSI ranging, and distinguishes the weights of the effective sampling nodes by RSSI ranging of the surrounding anchors and current neighbor nodes. In addition, an improved motion model which is conducive to the prediction of the node's motion direction is proposed.

The rest of the paper is organized as follows. Section 2 discusses the related localization algorithm MCL and MCB. Section 3 introduces the proposed IMCB from the aspect of improvement ideas, optimization method of sampling weight based on RSSI and improved motion model for sampling prediction. Section 4 provides the simulation results of IMCB and analyzes the comparison to existing algorithms. Finally, section 5 concludes the paper.

## 2. Related Work

### 2.1. MCL Algorithm

MCL algorithm has the following assumptions: all nodes are movable and the time is divided into several discrete time slots with equal length, and the node position is updated once in each time unit; the unknown node only knows its maximum moving distance  $v_{\max}$  in unit time; the communication range of each node is  $r$ .

In the following description,  $l_t$  represents the position distribution of common nodes at time  $t$ .  $o_t$  represents the observation value sent by anchor nodes from  $t-1$  to  $t$ .  $L_t = \{l_t^0, l_t^1, \dots, l_t^{48}, l_t^{N-1}\}$  represents the possible position sampling set of nodes at time  $t$ , including  $N$  samples.  $p(l_t | l_{t-1})$  represents the prior probability of unknown node predicting the position at current time based on the previous time.  $p(l_t | o_t)$  represents the posterior probability of  $l_t$  obtained based on the observation value  $o_t$ . MCL algorithm is divided into four phases: initialization, prediction, filtering and locating.

(1) Initialization: Each common node constructs a sampling set of its own possible positions  $L_t = \{l_t^0, l_t^1, \dots, l_t^{48}, l_t^{N-1}\}$ .

(2) Prediction: The common node extracts a new sampling set  $\bar{L}_t$  from the position information  $\bar{L}_{t-1}$  and motion information of the previous moment. Then the possible node position at the current time is in the circular area  $C_v$  with the center of  $l_{t-1}^i$  and the radius of  $v_{\max}$ . The samples in the circle are uniformly distributed:

$$p(l_t | l_{t-1}) = \begin{cases} \frac{1}{\pi v_{\max}^2} & d(l_t, l_{t-1}) < v_{\max} \\ 0 & d(l_t, l_{t-1}) \geq v_{\max} \end{cases} \quad (1)$$

(3) Filtering: At this phase, according to the observation values of one hop and two hop anchor nodes received, common node filters the invalid position samples in  $\bar{L}_t$ , the one-hop neighbor node receiving the message should be in the circle with the anchor node as the center and  $r$  as the radius, while the two-hop neighbor node should be in the circle with the anchor node as the center and the radius of  $(r, 2r)$ , and the position sampling that does not meet the condition is invalid sampling, that is:

$$p(l_t | o_t) = \begin{cases} 1 & \forall s \in S, d(l, s) \leq r \wedge \forall s \in T, r < d(l, s) \leq 2r \\ 0 & \text{others} \end{cases} \quad (2)$$

Where  $s$  represents an anchor node,  $S$  represents a set of one-hop anchor nodes, and  $T$  represents a set of two-hop anchor nodes. In order to obtain enough position samples, when the invalid samples in the sample set are filtered out, the previous prediction and

filtering process are repeated until the number of samples is met or the upper limit of sampling rounds is reached.

(4) Locating: Finally, the estimated position  $es\_p_t$  of the common node is the average value of the sample set, where the weight  $w_t^j$  of the sample point is equal to 0 or 1.

$$es\_p_t = \frac{\sum_i l_t^i w_t^i}{\sum_i w_t^i} \quad (3)$$

## 2.2. MCB Algorithm

MCB algorithm is an improved method to solve the problem of low efficiency and long computation time caused by the ambiguity of sampling range of MCL algorithm, that is, the communication range of anchor nodes is used to constrain sampling area. In the MCB algorithm, for convenience, a circular communication domain with the anchor node  $S$  as the center and the communication distance  $r$  as the radius is approximated as a circumscribed square of the circle with the anchor node  $S$  as the center and  $2r$  as the side length, called the anchor box. If a two-hop anchor node is used, the side of the anchor box is  $4r$ . The other phases of the MCB algorithm are the same as the MCL algorithm, but the anchor node sampling box is established during the sampling phase, as shown in Fig.1. Sampling in the overlapping area of these anchor boxes can effectively narrow the sampling range, improve the sampling efficiency and quality, shorten the positioning time, reduce the calculation amount, and improve the positioning speed and accuracy.

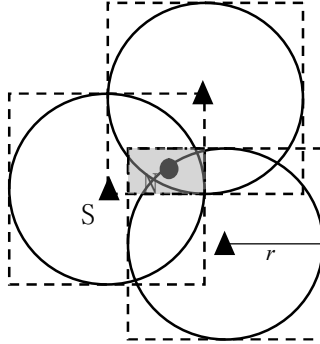


**Fig.1.** Sampling in the overlapping area of the anchor boxes can effectively narrow the sampling range

The anchor node sampling box is a circumscribed square overlapping area in which the anchor node  $S$  is the center of the circle and the communication range  $r$  is a radius. This area can be expressed as follows:

$$\begin{cases} x_{\min} = \max_{j=1}^n (x_j - r) \\ x_{\max} = \min_{j=1}^n (x_j + r) \\ y_{\min} = \max_{j=1}^n (y_j - r) \\ y_{\max} = \min_{j=1}^n (y_j + r) \end{cases} \quad (4)$$

Where  $x_{\min}, x_{\max}, y_{\min}$  and  $y_{\max}$  are the coordinate range of the sampling box,  $n$  is the number of anchor nodes, and  $x_j, y_j$  are the horizontal and vertical coordinates of the  $j$ -th anchor point. Fig. 1 and (4) show the case of a one-hop anchor node. If a two-hop anchor node is used, in the above figure and (4),  $r = 2r$ . The velocity sampling box at the previous moment is constructed in the same way as the MCL algorithm, and then the intersection of the two boxes is sought.

### 3. An Improved MCB Algorithm Based on weighted RSSI and motion prediction

#### 3.1. Improved MCB Algorithm

Although, the MCB algorithm limits the sampling range of position prediction by making full use of the information of one-hop (two-hop) anchor nodes that unknown nodes can "hear", and effectively improves the accuracy and efficiency of node positioning [10]. However, there are still some problems in MCB: firstly, MCB can get the final estimated position by averaging all sampling points, without effectively distinguishing good sampling points from bad ones; secondly, the motion models used in MCB and MCL algorithm are all improved Random Waypoint Mobility Models, the movement direction of nodes in each time unit are arbitrarily selected. However, in practice, the movement direction range of nodes should be limited.

In order to further improve the sampling efficiency of MCB algorithm and solve the above two problems, this paper proposes the scheme which can further reduce the sampling area of unknown nodes by using the historical anchor nodes, optimize the weight of sample points in the sampling set by using the received signal strength indication information between the unknown nodes and the neighbor nodes, then dynamically predict the movement direction of nodes in the sampling phase.

Suppose that the anchor box has been established according to the steps described above, and the sampling area of the node position is reduced according to the anchor node information of the node to be located at time  $t-1$ , so as to further improve the sampling efficiency. As shown in Fig. 2 (a),  $n_{t-1}$  is the position of the node to be located at time  $t-1$ ,  $n_t$  is the position of the node to be located at time  $t$ , and  $s_{t-1}$  is the neighbor anchor node of the node to be located at time  $t-1$ . Because  $n_{t-1}$  must be in the communication range of  $s_{t-1}$ , that is,  $d(n_{t-1}, s_{t-1})$  must be less than  $r$ , and the

maximum moving distance of  $n_t$  is  $v_{\max}$ , so  $n_t$  must be in the circle with  $s_{t-1}$  as the center and  $r + v_{\max}$  as the radius.

As shown in Fig. 2 (b), the distance  $d_{r_{ss}}$  from  $n_{t-1}$  to  $s_{t-1}$  can be calculated by the received signal strength. According to the above principle,  $n_t$  can be limited to a circle with  $s_{t-1}$  as the center and  $d_{r_{ss}} + v_{\max}$  as the radius, further reducing the limit range of  $s_{t-1}$  to  $n_{t-1}$ . In this way, with reference to the method of MCB, the circumscribed square of the circle is established.  $X(s_{t-1}, j), Y(s_{t-1}, j)$  are the abscissa and ordinate of the  $j$ -th anchor node at time  $t-1$ , respectively. Then the overlap between the circle and the anchor box can be calculated as follows:

$$\begin{aligned} x_{\min} &= \max_{j=1}^m \{x_{\min}, X(s_{t-1}, j) - d_{r_{ss}} - v_{\max}\}, x_{\max} = \max_{j=1}^m \{x_{\max}, X(s_{t-1}, j) + d_{r_{ss}} + v_{\max}\} \\ y_{\min} &= \max_{j=1}^m \{y_{\min}, Y(s_{t-1}, j) - d_{r_{ss}} - v_{\max}\}, y_{\max} = \max_{j=1}^m \{y_{\max}, Y(s_{t-1}, j) + d_{r_{ss}} + v_{\max}\} \end{aligned} \quad (5)$$

After the sampling box has been established as above, position sampling can be carried out for the nodes to be located in the sampling box.

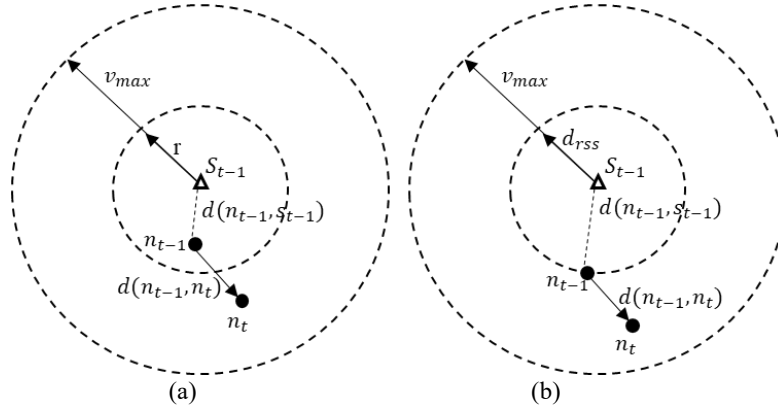


**Fig.2.** In order to further constrain the node position sampling area, the historical anchor node information and RSSI ranging results are used to limit the position sampling at the current time

In the filtering phase, common nodes filter the invalid position samples in  $L_t$  according to the observation values of one-hop and two-hop anchor nodes received. The basic method is the same as that of MCL algorithm, and then the restriction conditions of historical anchor nodes are added, namely:

$$p(l_t | o_t) = \begin{cases} 1 & \forall s \in S, d(l, s) \leq r \wedge \forall s \in T, r < d(l, s) \leq 2r, \\ & \wedge \forall s \in H, d(l, s) \leq r + v_{\max} \wedge \text{Meet motion model limitations} \\ 0 & \text{others} \end{cases} \quad (6)$$

Where,  $l$  represents the position sampling point,  $s$  represents an anchor node,  $S$  represents a set of anchor nodes,  $T$  represents a set of two anchor nodes, and  $H$  represents a set of historical anchor nodes. For the limitations of the motion model on the sampling points, see section 3.3. In order to obtain enough position samples, when the invalid samples in the sample set are filtered out, the previous predictive sampling and filtering process are repeated until the number of samples is met or the upper limit of sampling rounds is reached.

### 3.2. Optimization of sampling weight based on RSSI

In the actual wireless communication, the surrounding environment is very complex. The reflection, diffraction and scattering of electromagnetic wave will cause the signal fading. In the system simulation, the lognormal shadow fading model is often used to characterize the channel characteristics, and the formula is as follows:

$$P_r(d) = P_r(d_0) - 10n \lg \frac{d}{d_0} + X_\sigma \quad (7)$$

Where,  $P_r(d)$  is the received signal strength at the distance  $d$ ,  $P_r(d_0)$  is the received signal strength at the reference distance  $d_0$ , and  $n$  is the path loss exponent, which represents the path loss rate. In free space,  $n=2$ .  $X_\sigma$  is a random variable with Gaussian distribution of zero mean, and its standard deviation is  $\sigma$  in dB. According to formula 7, the propagation distance of the signal can be calculated according to the received signal strength of the node, and the calculated value can be used to approximate the real distance between nodes.

In this paper, RSSI ranging is used to estimate the distance between the node to be located and its one hop anchor node, which is stored by the node to be located. When positioning, it is necessary to obtain the distance  $d_{rss}$  between the node to be located and its historical anchor node at  $t-1$  time. If the distance between node  $i$  to be located and one hop anchor node  $j$  obtained by RSSI ranging is  $\hat{d}_{ij}$ , for practical consideration, this distance cannot exceed the communication range, and the its value can be estimated as:

$$d_{rss} = \min(\hat{d}_{ij}, r) \quad (8)$$

This distance will be used to limit the position sampling area of the node to be located. The position estimation based on RSSI weight can be divided into two stages: the non-weighted position estimation and the weighted position estimation. In the first stage, the common node obtains the average position estimation according to the filtered effective sampling points, and sends the value and its position error estimation to the common neighbor node; in the second stage, the common node calculates the weight through the RSSI distance according to the neighbor anchor node information, the neighbor node's

position estimation and its position error estimation, and updates the estimated position. The RSSI weights are calculated as follows:

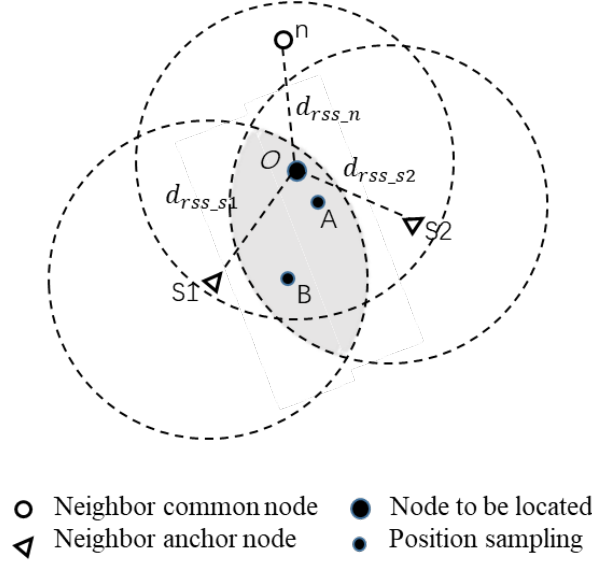


**Fig.3.** Computing sample weights according to the neighbor nodes' RSSI

As shown in Fig.3,  $O$  is the node to be located,  $S1$ ,  $S2$  and  $n$  are two anchor nodes and one common node within the communication range of the node to be located. The intersection of circle  $S1$  and circle  $S2$ , namely the shadow part, is the effective range of  $O$  position sampling, and  $A$  and  $B$  are the two position sampling within the effective range. The distance between the unknown node and the anchor node and the neighbor node can be estimated by the signal RSSI received by the unknown node, which is labeled  $d_{rss\_s1}$ ,  $d_{rss\_s2}$  and  $d_{rss\_n}$ .

The distance from the sampling point to the anchor node can be calculated according to the known coordinates. The distance from the sampling point to the common neighbor node can be approximated by the non-weighted estimated distance from the sampling point to the neighbor node, marked as  $d(l_i^i, s1)$ ,  $d(l_i^i, s2)$  and  $d(l_i^i, n)$ . Considering the errors of RSSI ranging and neighbor node position estimation, RSSI ranging error factor  $\delta_{rss_i}$  ( $\delta_{rss_i} > 0$ ) and neighbor node position error estimation  $ER_n$  are added to the weight calculation. The weight calculation method is: if  $l_i^i$  satisfies three inequalities in equation (9) at the same time, then the weight  $\omega_i^i$  of  $l_i^i$  plus 1. For example, the weight of position sampling  $A$  in Fig.3 is greater than that of  $B$ .

$$\begin{cases} |d_{rss\_s1} - d(l_i^i, s1)| < \delta_{rss_i} \\ |d_{rss\_s2} - d(l_i^i, s2)| < \delta_{rss_i} \\ |d_{rss\_n} - d(l_i^i, n)| < ER_n + \delta_{rss_i} \end{cases}$$

The computing method of  $ER_n$  is as follows: Establish a minimum rectangular box for the filtered effective sampling points, so that all the effective sampling points can be included, as shown in Fig.4. Point  $es\_p$  is the estimated position of all the effective position sampling points after the non-weighted average. The variables  $dx$  and  $dy$  are the maximum errors of the sampling points in X and Y directions, then:

$$ER_n = \sqrt{dx^2 + dy^2} \quad (10)$$

1. When there are three or more anchor nodes in the range of the unknown node, only anchor nodes are taken for the weight computing of position sampling;
2. If the number of anchor nodes in the communication range of the unknown node is less than three, the neighbor nodes with the smallest  $ER_n$  are used to supplement the number, and then neighbor anchor nodes and common nodes are used for the weight computing of position sampling;
3. If the total number of neighbor anchor nodes and common nodes is less than three, no weight computing will be carried out, and the result of non-weighted position estimation in the first stage will be taken as the position estimation of unknown nodes.

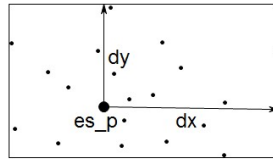


Fig.4. Computing the Estimation of Localization Error, where black dots represent all valid position samples of a neighbor's common node

### 3.3. Optimization of sampling prediction based on motion model

The basic idea of the sampling prediction optimization is that the motion model restricts the motion direction of the nodes, and the prediction sampling points of the unknown nodes should also be limited within the range of the possible motion direction.

#### Improvement of motion model

The motion model used in MCL algorithm simulation is an improved random middle point motion model, which takes the current position of the node as the starting position, selects any position within the deployment area of the node as the destination position to determine the movement direction of the node, and uses any value within the range (minimum rate, maximum rate) as the movement rate of the node to move towards the destination position. The algorithm considers that the motion in different time slots is independent of each other, which may cause some unrealistic motion behaviors of

nodes, such as sharp turning 180 degrees. Therefore, this paper improves the motion model of the node on the basis of the random middle node motion model, and limits the motion direction of the node to a realizable range, that is, the angle between the motion direction of the node selected at the next moment and the original motion direction should be less than the maximum realizable angle. As shown in Fig.5,  $l_{t-2}$  and  $l_{t-1}$  are the positions of the nodes in the first two moments respectively, and  $l_t$  is the position where the nodes are about to arrive.  $\alpha$  is the angle between vector  $l_{t-1}l_t$  and  $l_{t-2}l_{t-1}$ , which represents the steering angle of node motion, and  $\Delta\phi$  is the maximum value of  $\alpha$ . Therefore,  $\alpha$  is limited to  $\Delta\phi$ , which avoids the unrealistic too large steering angle of the node in the process of motion.

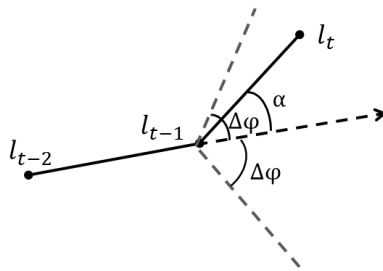


**Fig.5.** Modifying motion model which can limit the motion direction of the node by setting the maximum angle  $\alpha$ .

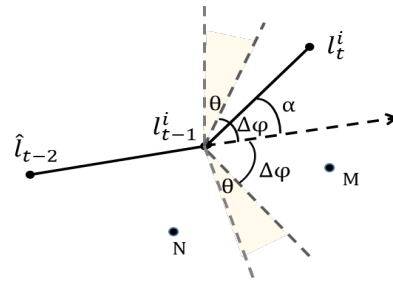


**Fig.6.** Predicting direction based on motion model and filtering the invalid nodes.

### Optimization of sampling point prediction based on motion model

On the basis of the above improved motion model, this paper predicts the dynamic motion direction of nodes based on the number of anchor nodes in the sampling phase, that is, the sampling is only in the range of possible motion direction of nodes. Fig. 6 is a direction prediction model for node position prediction sampling, in which  $\hat{l}_{t-2}$  is the node position estimation at time  $t-2$ ,  $l_{t-1}^i$  is the  $i$ -th position sampling of the node at time  $t-1$ ,  $l_t^i$  is the  $i$ -th position sampling of the node at time  $t$ , where  $i \in [0, N-1]$ ,  $N$  is the maximum number of samples in the unknown node position sampling set. Because  $\hat{l}_{t-2}$  and  $l_{t-1}^i$  are estimated information and have errors with the real positions of nodes in the first two moments, angle  $\theta$ , the correction angle of  $\Delta\phi$ , is added to the direction prediction model. For the convenience of the following description, the vector with  $\hat{l}_{t-2}$  as the starting point and  $l_{t-1}^i$  as the end point is recorded as vector  $\mathbf{a}$ ; the vector with  $l_{t-1}^i$  as the starting point and  $l_t^i$  as the end point is recorded as vector  $\mathbf{b}$ , then the angle between  $\mathbf{a}$  and  $\mathbf{b}$  cannot exceed the maximum steering angle  $\Delta\phi$ .

Define the estimated maximum steering angle  $\Delta\phi$  as the sum of the actual maximum steering angle  $\Delta\varphi$  and the correction angle  $\theta$  :

$$\Delta\phi = \Delta\varphi + \theta \quad (11)$$

$$\theta = \frac{1}{m_{t-2}m_{t-1}\sigma_1 + n_{t-2}n_{t-1}\sigma_2 + k} \times \delta \quad (12)$$

$$\sigma_1 + \sigma_2 = 1 \quad (13)$$

Among them,  $m_{t-2}$  and  $m_{t-1}$  are the number of anchor nodes in the communication range of unknown nodes at time  $t-2$  and  $t-1$  respectively,  $n_{t-2}$  and  $n_{t-1}$  are the number of two hop anchor nodes at time  $t-2$  and  $t-1$  respectively,  $\sigma_1$  and  $\sigma_2$  respectively represent the influence ability of one-hop anchor node number and two-hop anchor node number on localization error. The more the number of anchor nodes in the communication range of unknown nodes, the smaller the localization error of  $\hat{l}_{t-2}$  and  $\hat{l}_{t-1}$ , the smaller the correction angle  $\theta$ , otherwise  $\theta$  is larger;  $k$  is a constant, its function is to avoid zero denominator;  $\delta$  is a settable parameter with unit "degree". As shown in Fig.6,  $M$  is the effective sampling points and  $N$  is filtered points.

#### 4. Simulation and analysis

In order to effectively evaluate the performance of the improved Monte Carlo localization boxed algorithm (IMCB) proposed in this paper and compare its performance with MCL and MCB, we build a network simulation platform [9]. The platform uses JAVA as the development environment, and the simulation parameters are set as follows:

The entire simulation area is a square area  $A$  of  $500m \times 500m$ , and 320 nodes generated by each simulation are randomly distributed including several anchor nodes, and the rest are common nodes. The node moves randomly in the deployment area according to the improved motion model as above, and the actual maximum steering angle is  $\Delta\varphi = 60^\circ$ .

In the direction prediction, set  $\sigma_1 = 0.8$ ,  $\sigma_2 = 0.2$ ,  $k = 1$  and  $\delta = 120^\circ$ , that is, when  $m_{t-2}m_{t-1}\sigma_1 + n_{t-2}n_{t-1}\sigma_2 = 0$ , the maximum steering angle  $\Delta\phi = \Delta\varphi + \theta = 180^\circ$  is estimated because the accuracy of the reference direction is too low. The  $v_{\max}$  is the maximum moving speed of the node, which represents the maximum moving distance of the node in each time unit. When the motion model is adopted, the node is randomly selected from  $(0, v_{\max})$ ,  $s_d$  is the density of anchor nodes, which represents the average number of anchor nodes in the range of one hop communication.

$$s_d = \frac{\text{anchor\_num}}{A} \times \pi r^2 \quad (14)$$

Where  $anchor\_num$  is the total number of anchor nodes in the deployment area,  $A$  is the total area of the deployment area, and  $r$  is the communication radius of the node.

#### 4.1. Localization error

The localization error of the node is denoted by the distance between the estimated position coordinate of the node and the real position coordinate. The computing method is as follows:

$$error = \frac{\sum_{i=0}^{num} \sqrt{(x'_i - x_i)^2 + (y'_i - y_i)^2}}{num \times r} \quad (15)$$

Where  $(x_i, y_i)$  is the real coordinate of node  $i$ ,  $(x'_i, y'_i)$  is the node location coordinate computed by the location algorithm,  $num$  is the number of deployed common nodes, and  $r$  is the communication radius of the node.

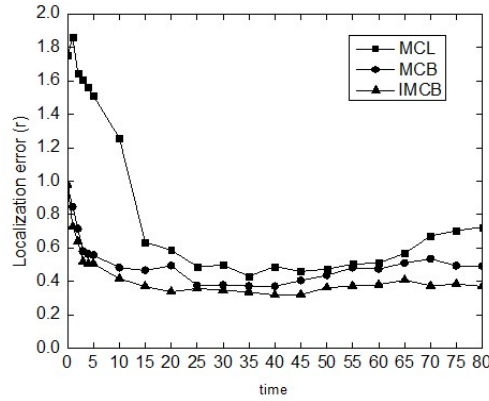


Fig.7. Localization error over time when  $v_{max} = 0.2r$ ,  $S_d = 1$

Fig.7 shows the curve of node localization error over time when  $v_{max} = 0.2r$  and  $S_d = 1$ . The localization of nodes can be divided into initialization stage and stabilization stage. In the initialization stage, the localization accuracy of all three algorithms is very poor. With the increase of time, the localization error decreases rapidly, and the IMCB and MCB algorithm reach the stable stage faster than MCL, and the localization error of IMCB is improved obviously. In addition, after the 45-th time unit, the localization error shows an upward trend. Due to the accumulation of errors, MCL is easy to lead to the insufficient number of node positioning prediction samples, and the localization error continues to increase. On the contrary, due to the limitation of anchor box in position prediction, MCB and IMCB prevent the worse of node localization error. IMCB makes use of the limitation of historical anchor nodes and predicts the movement direction of the nodes, which further reduces the sampling range.

At the same time, RSSI weight optimization effectively distinguishes the possibility that the sample points are close to the real position, thus obtaining more accurate location accuracy than MCB. From the simulation results, the localization error of IMCB is 11.2% lower than that of MCB. If only the value of stabilization stage is estimated, the localization error of IMCB is 12.41% lower than that of MCB.

#### 4.2. Impact of maximum rate

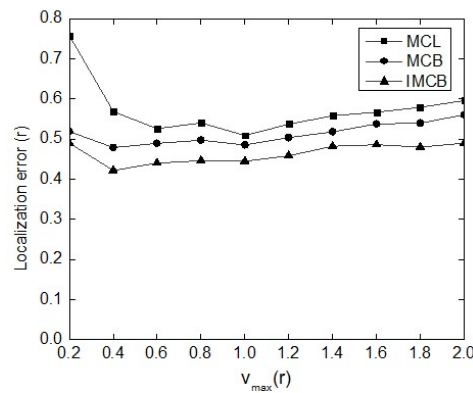


Fig.8. Impact of maximum rate when  $s_d = 1$

The increase of  $v_{max}$  will make the sampling area larger, but from another point of view, the rapid movement of nodes may bring more anchor node information. Fig.8 shows the curve of node localization error with node movement rate when  $s_d = 1$ . The error value is the average error after multiple localization of the specified  $v_{max}$ . It can be seen that with the increase of  $v_{max}$ , the localization error decreases significantly between  $0.2r$  and  $0.4r$ . After that, the localization errors of MCB and MCL have an obvious upward trend. Although the localization errors of the IMCB algorithm is also increase, the trend is obviously slow. This is because the sampling range of MCB and MCL position prediction will increase with the increase of  $v_{max}$ . But for IMCB, in addition to the limitation of anchor box and  $v_{max}$ , direction prediction is also added, which is independent of  $v_{max}$ . When  $v_{max}$  increases to the extent that it is ineffective to predict the sampling range of the limited position, that is to say, when the square constructed according to  $v_{max}$  completely covers the anchor box, the range limitation impact of the direction prediction is still effective. Therefore, with the increase of  $v_{max}$ , the rising trend of IMCB localization error is smooth, and the location accuracy is better than that of MCB.

### 4.3. Impact of anchor node density

Increasing the density of anchor nodes is beneficial for reducing the localization error, but it will undoubtedly increase the deployment cost of the network. Fig.9 shows the curve of localization error changing with the density of anchor nodes when  $v_{\max}=0.2r$ . It can be seen from the figure that the localization error of IMCB is lower than that of MCB. On the one hand, the increase of the number of anchor nodes makes the weight optimization based on RSSI more effective. On the other hand, the increase of anchor nodes improves the location accuracy, and also makes the range of direction prediction angle smaller in the next positioning, thus reducing the range of position prediction and further improving the location accuracy. In addition, the constraints of historical anchor nodes make the location accuracy of IMCB due to MCL and MCB when the density of anchor nodes is low.

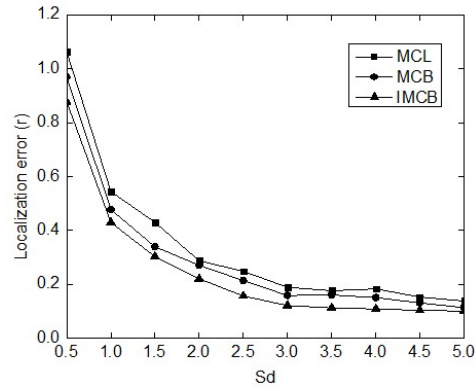


Fig.9. Impact of anchor node density where  $v_{\max}=0.2r$

## 5. Conclusion

Location problem is one of the hotspots in wireless sensor network research. In order to further improve the performance of the MCL algorithm which has attracted much attention in the field of mobile sensor network in recent years, this paper designs a weighted localization algorithm named Improved Monte Carlo Localization Boxed (IMCB) based on the historical anchor node and RSSI ranging, which has the following advantages: firstly, using the historical anchor node and the historical RSSI ranging information to further narrow the sampling range of the unknown node, improve the sampling efficiency of the node position, and also to some extent alleviate the problem of anchor node density; Secondly, the weight optimization based on RSSI effectively distinguishes the weight of the sampling points, which is conducive to further reducing the localization error of the nodes; thirdly, the improvement of the motion model is

beneficial to the direction prediction of the nodes, reducing the sampling range of the position prediction, improving the localization efficiency and accuracy of the nodes. However, there are still many factors affecting the location algorithm, such as computational complexity, location time, environmental disturbance, network security, etc. which will affect the performance and conditions for use of the algorithm. More in-depth research and evaluation are needed.

**Acknowledgment.** The authors wish to acknowledge the Beijing Municipal Natural Science Foundation of China (No. 4172045) for the support in funding this work.

## References

1. W. Cui, S. C. Wu, Y. Z. Wang. A Gossip-Based AOA Distributed Localization Algorithm for Wireless Sensor Networks [J]. *Applied Mechanics and Materials*, 2014, Vol. 577: pp. 841-846.
2. M. Jamalabdollahi and S. Zekavat. Time of Arrival Estimation in Wireless Sensor Networks via OFDMA [C] // *Vehicular Technology Conference*. Boston, MA: IEEE, 2015, pp. 1-5.
3. Weile Zhang , Qinye Yin, Wenjie Wang. Distributed TDoA estimation for wireless sensor networks[C] // *Proceedings 2010 IEEE International Conference on Acoustics, Speech and Signal Processing*: 2010, p 2862-5.
4. F. Yaghoubi, A. A. Abbasfar and B. Maham. Energy-Efficient RSSI-Based Localization for Wireless Sensor Networks [J]. *IEEE Communications Letters*, June 2014, vol. 18, no. 6, pp. 973-976.
5. Laurendeau C, Barbeau M. Centroid Localization of Uncooperative Nodes in Wireless Networks Using a Relative Span Weighting Method[J]. *Eurasip Journal on Wireless Communications & Networking*, 2010, 2010(1):1-10.
6. Agashe A A, Agashe A A, Patil R S. Evaluation of DV Hop Localization Algorithm in Wireless Sensor Networks[C]// *International Conference on Advances in Mobile Network, Communication and ITS Applications*. 2012:79-82.
7. P. Ren, W. Liu, D. Sun and K. Liu. Node Localization based on Convex Optimization in Wireless Sensor Networks [C]// *Fuzzy Systems and Knowledge Discovery (FSKD)*, 12th International Conference. Zhangjiajie: IEEE, 2015: 2169-2173.
8. Zhang Aiqing, Ye Xinrong, Hu Haifeng. Point in triangle testing based trilateration localization algorithm in wireless sensor networks [J]. *Internet and Information Systems*, 2012, vol.6: 2567-2586.
9. Hu L, Evans D. Localization for mobile sensor networks [J]. *Wireless Communication*, 2004:45--57.
10. Aline Baggio , Koen Langendoen . Monte-Carlo Localization for Mobile Wireless Sensor Networks . *Lecture Notes in Computer Science* , 2006 , 4325 (1 1):317-328.
11. Dil B,Dulman S,Havinga P. Range-based localization in mobile sensor networks [J]. *Wireless Sensor Networks*, 2006: 164-179.
12. Wang W D, Zhu Q X. RSS-based Monte Carlo localisation for mobile sensor networks [J]. *Communications, IET*, 2008, 2(5): 673-681.
13. Baggio and K. Langendoen. Monte-Carlo Localization for Mobile Wireless Sensor Networks [C]// *Mobile Ad-Hoc and Sensor Networks* , 2006: 317-328.
14. P. Wang, N. Chen, F. Zha, W. Guo and M. Li, "Research on Adaptive Monte Carlo Location Algorithm Aided by Ultra-Wideband Array," 2018 13th World Congress on Intelligent Control and Automation (WCICA), Changsha, China, 2018, pp. 566-571.

15. J. Luan, R. Zhang, B. Zhang and L. Cui. An Improved Monte Carlo Localization Algorithm for Mobile Wireless Sensor Networks [C]// Computational Intelligence and Design (ISCID), 2014 Seventh International Symposium. 2014: 477-480.
16. P. Li, Y. Zhang and Q. Zhang, "Monte Carlo Location Algorithm Based on Model Prediction," 2018 International Symposium in Sensing and Instrumentation in IoT Era (ISSI), Shanghai, 2018, pp. 1-5.
17. W. Chen, T. Huang and A. Maalla, "Research on Adaptive Monte Carlo Location Method Based on Fusion Posture Estimation," 2019 IEEE 3rd Advanced Information Management, Communicates, Electronic and Automation Control Conference (IMCEC), Chongqing, China, 2019, pp. 1209-1213.

**Chunyue Zhou** completed her BSc in Information Engineering, MSc and PhD in Communication & Information Systems from the School of Electronic and Information Engineering, University of Beijing Jiaotong, China. She has been working in the areas of network technology and security for many years. She is now a Senior Engineer and her research interests include the next generation Internet and information security.

**Hui Tian** is a Senior Lecturer and the Discipline Head of Computer Science in Griffith University. She has been working in the areas of network analysis and optimization, privacy and security for over 15 years. Her contributions to research range from network topology discovery, routing protocols in wireless sensor networks to the challenging issues about data publishing in social networks with privacy preservation, anomaly detection in network traffic analysis and other security issues in networks.

**Baitong Zhong** completed his BSc in Electronic & Information Engineering from the Northeast Petroleum University, MSc in Information Technology from the School of Computer Science and Information Technology, University of RMIT, Australia. He is now a teaching assistant in Hunan Electronic Technology Vocational College and his research interests include the IOT technology and information security.

*Received: February 04, 2020; Accepted: July 15, 2020*